(1987); *J. Mater. Sci.* **20**, 1321 (1985); J. E. Marion, C. H. Hsueh, A. G. Evans, *J. Am. Ceram. Soc.* **70** [10], 708 (1987).
18. The authors thank A. G. Evans, F. F. Lange, R. M. McMeeking, M. Rühle, H. Vydra, and N. Derry for constructive comments. J.N.I. and P.M.McG. thank the office of Naval Research for financial support under contract N0014-87-K-0013 and A.M.H. thanks IBM Research Labs for sabbatical leave support.

15 January 1988; accepted 25 February 1988

Tertiary Structure Is a Principal Determinant to Protein Deamidation

A. A. KOSSIAKOFF

The protein deamidation process involves the conversion of the amide side-chain moieties of asparagine and glutamine residues to carboxyl groups. This conversion is an unusual form of protein modification in that it requires catalysis by an intramolecular reaction where both the substrate (asparagine and glutamine side chains) and "catalytic site" (the peptide nitrogen of the succeeding residue) are constituents of several consecutive residues along the polypeptide chain. The stereochemical factors governing this process were studied with a data base derived from the neutron crystallographic structure of trypsin from which amide groups and oxygen can be unambiguously differentiated because of their different neutron scattering properties. The neutron structure allowed for the direct determination of those residues that were deamidated; 3 of 13 asparagine residues were found to be modified. These modified residues were clearly distinguished by a distinct local conformation and hydrogen-bonding structure in contrast to those observed for the other asparagine residues. No correlation was found between preference to deamidate and the chemical character of residues flanking the site, as had been proposed from previous peptide studies.

DEAMIDATION OF ASPARAGINE RESidues is a commonly observed form of post-translational protein modification (*1–3*). The process may play an essential role in the degradation and clearance of proteins and may be under genetic control through sequence variation to adjust rates of degradation (*4–6*). The generally accepted mechanism of deamidation involves the formation of an intramolecular cyclic imide intermediate that can break down to replace the amide substituent group with a carboxyl group. The breakdown can proceed by either of two distinct pathways (Fig. 1) to form either a normal peptide linkage (that is, Asn to Asp) or a β-carboxyl linkage (*7*). Peptide studies have shown that glutamine can also undergo deamidation, but at much reduced rates (*2*).

Studies attempting to identify the stereochemical factors affecting deamidation have centered on the use of synthetic peptides and focused on the role that particular sets of flanking side-chain types (that is, X-Asn-Y) have on the process (*1, 4*). However, in the native folded state of the protein, tertiary structure would be expected to affect significantly the susceptability of amide side chains to undergo modification. In this study structural features were identified that affected the deamidation process and an attempt has been made to determine the relative importance of sequence versus conformational factors in promoting this type of intramolecular modification. Trypsin represents an excellent system to study because the sequences and conformations of the adjacent segments of polypeptide chain containing the asparagine residues show significant diversity.

Detailed studies of the interrelation between structural factors and deamidation have been limited because of the difficulties involved in identifying modified groups. Neutron diffraction, by virtue of its ability to observe hydrogen and deuterium atoms in large biomolecules, is ideally suited to identify deamidated residues in proteins. The interpretation of the state of amidation of Asn side chains in trypsin (*8*) was drawn from data taken from two highly refined neutron structures: a D_2O structure (the crystal was soaked in D_2O to exchange waters of crystallization and labile protons), $R = 0.190$ at 1.8 Å resolution, and a H_2O structure, $R = 0.197$ at 2.1 Å resolution (*9*). In a D_2O structure, the large scattering differences between oxygen (5.8 fermi) (*10*) compared with a nitrogen and two deuteriums (22.2 fermi) make the assignment of the orientation of amide side chains unambiguous (*9*). In the D_2O-trypsin analysis, 10 of the 13 well-ordered amide side chains refined to give reasonable temperature factor values (*11*) for all atoms. However, for Asn^{48}, Asn^{95}, and Asn^{115}, the temperature factors for the two side-chain deuterium atoms were greater than 80 $Å^2$ (these atoms have essentially no scattering contribution) compared with an average of about 15 $Å^2$ for the other side-chain atoms in these groups. A comparison of the structure around these asparagines to other asparagines and other side-chain groups with bonded deuteriums showed that the phasing model was of sufficient quality to have observed the deuteriums on the three Asp(Asn) side chains if they were present.

To further confirm these findings, the D_2O and H_2O structures were combined to calculate a D_2O-H_2O difference Fourier map, which is an extremely sensitive method for locating deuterium atoms (*12*). Because of the substantial scattering differences between hydrogen (−3.8 fermi) and deuterium (+6.6 fermi), amide groups produce large peaks in these difference maps; these maps are also less prone to phasing bias and effects due to partial exchange and disorder (*12*). Significant density was observed for the amide deuterium sites except for Asn^{48}, Asn^{95}, and Asn^{115}, which were nearly featureless (Fig. 2) (*13*). This result indicated that there were no exchangeable groups associated with these three side chains. This observation, together with the D_2O refinement results, offered extremely strong support for the interpretation that these asparagines had been deamidated.

An analysis of the conformational pattern and hydrogen-bonding interactions localized around Asn residues (Table 1) suggests

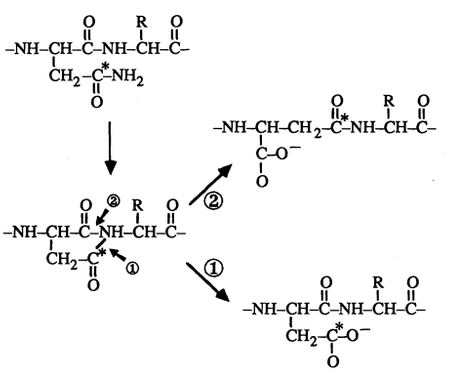

Fig. 1. Mechanism of deamidation: (i) Attack of the unprotonated peptide nitrogen of the $n + 1$ residue on the carbonyl carbon of the amide side chain; (ii) formation of a cyclic imide intermediate; (iii) attack by water at position 1 or 2 leading to a breakdown of the intermediate; (iv) formation of either the NH_2 to O substitution or the β-carboxyl insertion. The asterisk marks the position of the side-chain carbonyl carbon. In the β-carboxyl linkage, this carbon becomes part of the main chain and increases the chain length by one atom.

Department of Pharmaceutical Chemistry, University of California at San Francisco, San Francisco, CA 94143, and Department of Biomolecular Chemistry, Genentech, Inc., 460 Point San Bruno Boulevard, South San Francisco, CA 94080.

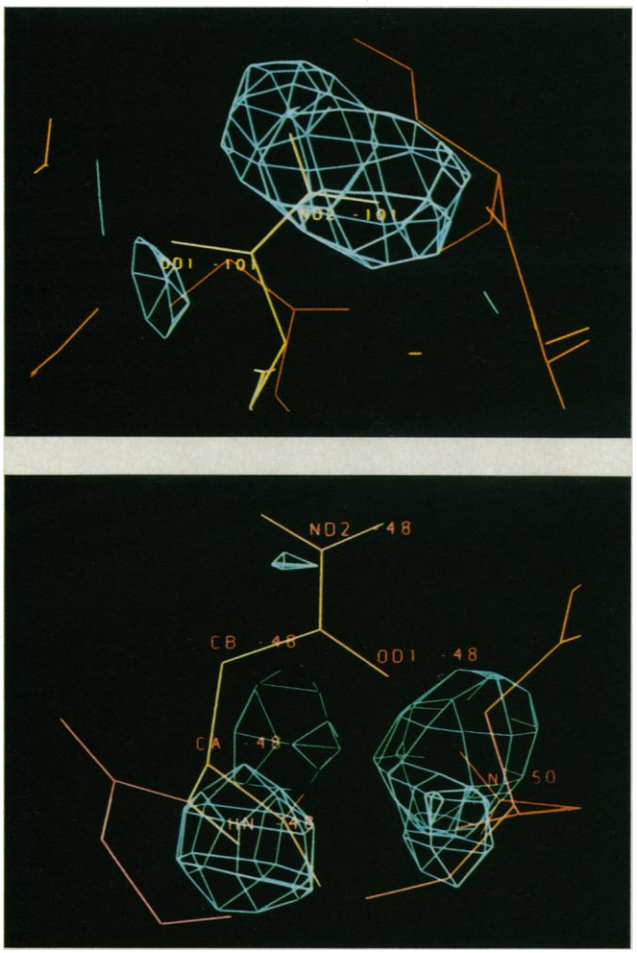

Fig. 2. Neutron D_2O-H_2O difference Fourier map showing representative density for: (**Top**) Asn^{101}, which was unmodified; and (**bottom**) a modified group (Asn^{48} to Asp). The observed density around the Nδ2 nitrogen atom of residue 48 is about 5 to 10% that expected for two exchanged protons. Density peaks not associated with the side chains of residues 48 and 101 are due to other exchangeable protons in the near vicinity of the groups.

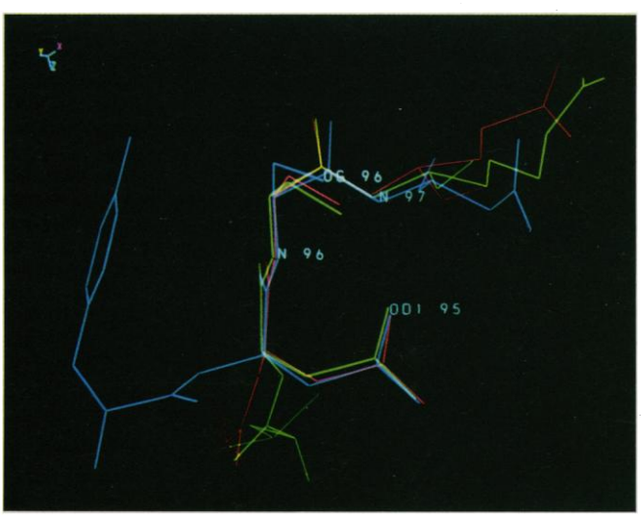

Fig. 3. Superimposed structures of residues 47 to 50 (red), 94 to 97 (blue), and 114 to 117 (green) showing close correspondence in conformations. The peptide chain preceding residue 95 has a different conformation than those of 48 and 115. Modeling suggested that, for residues 94 to 97, a larger conformational change is required to form the cyclic imide intermediate.

that several general structural features are responsible for deamidation. All three deamidated groups (48, 95, and 115) have similar main-chain and side-chain conformations (Fig. 3) characterized by the Oδ1 oxygen of the side chain forming a hydrogen bond with the peptide nitrogen that is two residues (n + 2) further in the sequence. This type of interaction is observed in conformations of peptide turns where an Asn group is found in the first position (*14*). The deviations in atomic positions when the observed conformations of 48, 95, and 115 have been superimposed are listed in Table 2. Note the close correspondence between the main-chain and the serine side-chain atoms, which, for the most part, is near the deviations expected for experimental error (0.2 to 0.3 Å).

Modeling showed that in these analogous conformations, with minimal main-chain movement (±20° phi, psi), the side chain can be rotated (80° around the Cα–Cβ bond) to place the amide carbonyl carbon in an orientation where it is readily accessible to attack by the peptide nitrogen of the succeeding (n + 1) residue (Fig. 4). In order for deamidation to occur, the n + 1 peptide nitrogen must be sterically accessible (as well as deprotonated); for instance, it should not be hydrogen bonded to any protein group. Another noteworthy aspect of the conformation of these groups is that in each case they are followed by a Ser residue with a side-chain orientation of $X1$ = +60° (*15*). This conformation places the Ser hydroxyl in a position to hydrogen bond to the Oδ1 oxygen or the Nδ2 hydrogen atoms (= 2.6 Å). In addition, the hydroxyl group could be oriented with small main-chain adjustments to hydrogen bond to the n + 1 peptide nitrogen, which may aid in the deprotonation of the nitrogen. These potential hydrogen bonds may facilitate the formation of the cyclic imide intermediate and possibly assist the reaction.

Although all of the deamidated groups in trypsin are conformationally similar, the example of Asn^{34} points out that a simple rule based on conformation alone cannot be applied to predict susceptibility to deamidation. Asn^{34} has a somewhat analogous conformation and side-chain hydrogen-bonding scheme to the three deamidated Asn residues and is followed by a Ser residue, but it shows no effects of modification. The principal feature that distinguishes it from those groups is that the succeeding peptide nitrogen is hydrogen bonded to a carbonyl oxygen (residue 39). Significant conformational change in this region would also be impeded by the hydrogen bond network: N34 to O64 and O34 to N64. Thus, based on steric and hydrogen-bonding constraints, this interaction would hinder formation of the productive deamidation geometry.

Modeling suggested that certain sets of peptide torsion angles are incompatible with deamidation. For example, in three cases, Asn^{25}, Asn^{101}, and Asn^{179}, a rotation of about 180° around the peptide bond would be required to produce a conformation similar to those of the deamidated sites. Even taking into consideration the intrinsic flexibility of proteins, flipping a peptide bond at these sites would necessitate extensive disruptions in the tertiary structure and likely would have large activation energies.

Structural constraints in the form of hydrogen bonds also probably play a role in protecting groups from deamidation. Residues 72 and 74 make up part of the highly structured Ca^{2+} binding loop of trypsin and are locked into restricted conformations. In

the cases of residues 34, 79, 97, 143, and 233, hydrogen bonds are made to their $n + 1$ peptide nitrogens that, as discussed above, should greatly hinder formation of a productive side-chain peptide nitrogen geometry required for deamidation. Hydrogen bonding of main-chain groups appears to inhibit deamidation more than whether the amide side chain itself is involved in a hydrogen bond—the side chains of all deamidated residues are hydrogen bonded, whereas those of three unmodified groups (79, 97, and 223) are not. Note that in cases where the hydrogen bond requires the side-chain amide moiety (Nδ2) as a donor (that is, for groups 74, 101, 179, and 233—see Table 1), or where multiple hydrogen bonds are made with the side chain, deamidation may be inhibited.

Table 1. Hydrogen-bonding interactions of Asn groups and their flanking residues. The hydrogen-bonding cutoff distance was 3.1 Å. Asn74 was the only group near an intermolecular crystal contact point.

Residue	Atom pairs		Distance (Å)
Asn^{25}	Oδ1 25	NH_2 117	2.6
Asn^{34}	Oδ1 34	N38	2.8
	Oδ1 34	Solvent	2.8
	O34	N64	2.9
	O34	Solvent	2.9
	N37	O39	2.9
	N34	O64	2.9
Asn^{48}	Oδ1 48	N50	2.8
Asn^{72}	Oδ1 72	N74	3.0
	N73	O153	3.0
	O72	Ca^{2+}	2.8
	N72	Oε2 77	2.8
Asn^{74}	Nδ2 74	Oδ1 153	2.6
	N74	Oδ1 72	3.0
	O74	Solvent	2.6
Asn^{79}	N80	Oε1 80	2.7
	N79	Oε1 80	3.1
Asn^{95}	N80	Oε1 80	2.7
	O95	N99	2.7
	N95	O100	2.9
	Oδ1 95	N97	2.7
Asn^{97}	N97	Oδ1 95	2.7
	N98	Oδ1 95	3.1
Asn^{100}	Oδ1 100	Oγ1 177	2.7
	Oδ1 100	Nδ2 179	2.9
	O100	N95	2.8
Asn^{101}	Oδ1 100	OH23	2.9
	Nδ2 101	O93	2.7
Asn^{115}	Oδ1 115	N117	2.8
	N115	O118	2.6
Asn^{143}	Oδ1 143	N150	2.8
	N144	O150	2.8
	N143	O192	2.7
	O143	N16	2.9
Asn^{179}	Oδ1 179	Nδ2 233	2.7
	Nδ2 179	Oδ1 100	2.9
	O179	N230	2.9
	O179	Solvent	2.6
Asn^{223}	N224	O221	2.8
	N223	O185	2.7
Asn^{233}	Nδ2 233	Oδ1 179	2.7
	Oδ1 233	Solvent	2.7
	N234	O231	2.8

Based on studies of peptides, it had been proposed that deamidation rates are governed primarily by the chemical character (steric and electronic) of the residues flanking the Asn group (*2*). The peptide data suggest that charged side chains increase rates of deamidation compared to neutral groups and that, within the neutral category, rates decrease with increasing size (that is, Gly > Ala > Val > Leu > Ile). The trypsin findings do not support the above interpretation as it applies to proteins. All three deamidated groups have the sequence X-Asn-Ser, where X is Ile^{47}, Tyr^{94}, and Leu^{114}, respectively. According to the peptide predictions, these large hydrophobic residues should retard deamidation. Asn^{34} has the identical sequence to Asn^{115}, Leu-Asn-Ser, yet is not modified. By arguments based on nearest neighbor effects, residues 25 (Ala-Asn-Thr), 72 (Ile-Asn-Asp), 79 (Gly-Asn-Thr), 97 (Ser-Asn-Asp), 101 (Asn-Asn-Asp), and 143 (Gly-Asn-Thr) should have deamidated more rapidly than residues 48, 95, and 115, which they do not. Based on proximity to the site of reaction ($n + 1$ peptide nitrogen), it is highly probable that the side chain of the $n + 1$ group plays a more important role in deamidation than does the side chain of the $n - 1$ residue. Certainly in those instances where the β-carboxyl linkage is formed, the size of the $n + 1$ side chain is a principal factor.

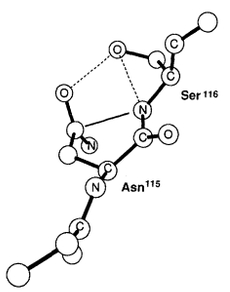

Fig. 4. Modeled conformation of the Asn^{115} side chain prior to attack by the peptide nitrogen of Ser^{116}. Orientation required rotation of about 80° around the Cα–Cβ side-chain bond with only small rotations (<20°) of the main-chain torsion angles (phi, psi). In this conformation the hydroxyl of Ser^{116} can hydrogen bond (2.6 Å) to the side Oδ1 or Nδ2. Since the formation of the imide intermediate is probably rate determining, this hydrogen bond is likely to be primarily with the Oδ1, effectively helping stabilize the partial negative charge that is generated on the oxygen. Another feature of the 116 hydroxyl orientation is that it may also be able to hydrogen bond to its peptide nitrogen (2.8 Å). This may assist in the deprotonation of the nitrogen. Similar models can be built for Asn^{95} and Asn^{48}.

Table 2. Deviations of the deamidated asparagines and their succeeding serine ($n + 1$) residue from the average of their superimposed structures. Experimental error in coordinates is about 0.2 to 0.3 Å.

Atom	Deviations from average conformation for various residues (Å)		
	48	95	115
	Asp		
N	0.7	0.5	0.8
Cα	0.2	0.3	0.1
Cβ	0.4	0.9	0.5
Cγ	0.3	0.5	0.1
C	0.1	0.2	0.1
O	0.2	0.3	0.1
	Ser		
N	0.1	0.1	0.1
Cα	0.1	0.1	0.1
Cβ	0.2	0.4	0.2
Cγ	0.1	0.5	0.4
C	0.1	0.1	0.1
O	0.1	0.2	0.1

The breakdown product of the cyclic imide intermediate to an aspartyl side chain cannot be distinguished by an x-ray analysis. However, if the β-carboxyl deamidation product were formed (Fig. 1), it would be readily distinguishable because of the alteration of the main-chain and side-chain lengths. To my knowledge there have been no reports in the crystallographic literature of the presence of a β-carboxyl linkage in proteins. This is somewhat surprising, because peptide studies indicate that formation of this breakdown product is not rare when the $n + 1$ residue is a Gly (or to a lesser extent other small groups, that is Ala or Ser) (*7*). It is also clear that β-carboxyl linkages are found in proteins (*16*). An enzyme, carboxyl methyltransferase, has been identified whose substrate is the β-aspartyl linkage and its presumed function is to facilitate repair or mark the site for further modification (*4, 5*). It is possible that β-carboxyls have not been identified in x-ray structures because they were not expected and therefore overlooked during model building, or that the groups were only partially modified, which would result in a mixture of structural species that were statically disordered in the crystal structure. Although the results presented were drawn from a limited data base and represent observations for folded proteins at a single *p*H (*p*H 7), structural criteria are probably important for the deamidation process in other protein systems as well.

REFERENCES AND NOTES

1. J. J. Harding, *Adv. Protein Chem.* **37**, 247 (1985).
2. A. B. Robinson and C. J. Rudd, *Curr. Top. Cell Regul.* **8**, 247 (1974); A. B. Robinson, J. W. Scotchler, J. H. McKerrow, *J. Am. Chem. Soc.* **95**, 8156 (1973).
3. T. J. Ahern and A. M. Klibanov, *Science* **228**, 1280 (1985); T. J. Ahern, J. I. Casal, G. A. Petsko, A. M. Klibanov, *Proc. Natl. Acad. Sci. U.S.A.* **84**, 675 (1987).

4. T. Geiger and S. Clarke, *J. Biol. Chem.* **262**, 785 (1987); S. Clarke, *Ann. Rev. Biochem.* **54**, 479 (1985).
5. B. A. Johnson and D. W. Aswad, *Biochemistry* **24**, 2581 (1985).
6. A. B. Robinson, J. H. McKerrow, P. Cary, *Proc. Natl. Acad. Sci. U.S.A.* **66**, 753 (1970).
7. E. D. Murray and S. Clarke, *J. Biol. Chem.* **258**, 10722 (1983); P. Bornstein and G. Balian, *Methods Enzymol.* **47**, 132 (1977); Y. C. Meinwald, E. R. Stinson, H. A. Scheraga, *Int. J. Peptide Protein Res.* **28**, 79 (1986).
8. It was not determined whether deamidation of the groups occurred prior to crystallization or during the period of crystal growth and data collection. Trypsin crystals grown to neutron size (4 mm^3) took approximately 1 year; subsequent soaking in D_2O and data collection took an additional 6 months. It is not expected that D_2O would greatly influence the deamidation process; analysis of the H_2O trypsin structure showed similar deamidation traits.
9. Experimental procedures are described in A. A. Kossiakoff and S. A. Spencer, *Biochemistry* **20**, 6462 (1981).
10. A fermi is a measure of the scattering capacity of a type of atom (such as hydrogen, nitrogen, or oxygen) toward neutrons and is similar to an x-ray form factor. Fermis are in units of scattering length, 10^{-13} cm.
11. Temperature factors measure the inherent vibratory motion of an atom defined as $B = 8\pi^2 \langle U^2 \rangle$ Å^2, where $\langle U^2 \rangle$ is the mean squared amplitude of atomic vibration.
12. J. Shpungin and A. A. Kossiakoff, *Methods Enzymol.* **127**, 329 (1986).
13. Integrated intensities at the Nδ2 deuterium sites of residues 48 and 95 were less than 10% the expected value for a fully exchanged site; for Asn^{115}, the densities were about 25% those of a full site.
14. J. S. Richardson, *Adv. Protein Chem.* **34**, 167 (1981).
15. *X*1 is a torsion angle defining the angular rotation of the hydroxyl group around the Cα–Cβ bond.
16. D. W. Aswad, *J. Biol. Chem.* **259**, 10714 (1984); B. A. Johnson, E. D. Murray, S. Clarke, D. B. Glass, D. W. Aswad, *ibid.* **262**, 5622 (1987).
17. The author acknowledges the technical assistance of J. Shpungin and thanks B. Schoenborn and his colleagues, who developed the neutron diffraction station at the Brookhaven High Flux Beam Reactor, and R. Wetzel for his suggestions during preparation of the manuscript.

16 November 1987; accepted 18 February 1988

Electric Field X-ray Scattering Measurements on Tobacco Mosaic Virus

M. H. J. Koch, E. Dorrington, R. Kläring, A. M. Michon, Z. Sayers, R. Marquet, C. Houssier

The feasibility of electric field x-ray solution scattering with biological macromolecules was investigated. Electric field pulses (1.25 to 5.5 kilovolts per centimeter) were used to orient tobacco mosaic virus in solution (4.5 milligrams per milliliter). The x-ray scattering is characteristic of isolated oriented particles. The molecular orientation and its field-free decay were monitored with a time resolution of 2 milliseconds by means of synchrotron radiation and a multiwire proportional area detector. The method should also be applicable to synthetic polymers and inorganic colloids.

It has been known at least since the beginning of the century (*1*) that electric fields affect light scattering. Light scattering in the presence of electric fields has been used to obtain information on a variety of materials ranging from viruses and nucleic acids to synthetic polymers and clays [for a review, see (*2*)]. Full use of the method requires particles sufficiently large, or a wavelength sufficiently short, for the scattering to be influenced by internal interference effects. The small ratio of particle size to wavelength and the strong absorption by samples are usually the limiting factors in electric field light scattering. These limitations can in principle be overcome by using x-rays.

X-ray electric field scattering should have two advantages, the first being the ability to study the effects of electric fields on macromolecules, thus bridging the gap between structural and electrooptical methods [for an introduction, see (*3*)]. The second would be the possibility of obtaining at least transiently, even with dilute systems, a partially oriented scattering pattern. It is mainly this second possibility that prompted us to perform the feasibility experiments described below, because there is some advantage in the study of fibrous systems like chromatin (*4*) in being able to unequivocally assign specific features of the solution scattering patterns to meridional or equatorial contributions in the pattern of oriented specimens. As an obvious test object for these experiments we chose tobacco mosaic virus (TMV), which is perhaps the system most thoroughly studied by electric dichroism and birefringence (*5–8*) and electric field light scattering (*9*). Furthermore, magnetic field orientation methods (*10, 11*) have been used on very concentrated TMV samples that display liquid crystalline behavior.

The x-ray scattering measurements were carried out on the X33 camera of the European Molecular Biology Laboratory (EMBL) in the Hamburg Synchrotron Laboratory (HASYLAB) (*12*) on the storage ring DORIS of the Deutsches Elektronen Synchrotron (DESY) at Hamburg.

The solution of TMV (4.5 mg/ml) in a buffer with 0.3 m*M* NaCl, 0.2 mM tris-HCl (*p*H 7.5), 3 m*M* EDTA, and 0.5 m*M* phenylmethylsulfonyl fluoride (PMSF) was contained in a cell with platinum electrodes (*13*). Electric field pulses (1.25 to 5.25 kV/cm) produced by a power pulse generator triggered by the data acquisition system (*14, 15*) were applied to the electrodes of the measurement cell. Two types of multiwire proportional detectors with delay-line readout (*16*) were used. The first is a quadrant detector (*17*) that integrates the scattering pattern azimuthally in one quadrant. This detector was placed alternately with the bisector of the quadrant along the field and perpendicular to the field and used to collect sequences of 128 time frames of 2 msec each. The second is an area detector with 256 by 256 elements, a resolution of 1 mm, and a dead time of 470 nsec (*18*).

Unipolar pulses were applied for 2 msec and the polarity was reversed before each new pulse. X-ray scattering data were accumulated for a series of 20 pulses, processed, and checked for degradation of the response of the sample. Damage to the samples could largely be eliminated by using bipolar pulses and a fast shutter to protect the samples from radiation between measurements. The same data acquisition system can be used for optical measurements (*19*).

Figure 1A illustrates the x-ray solution scattering pattern of a TMV solution under normal conditions. The shape of the scattering curves at low angle indicates that, under the conditions used, there is some polydispersity, but the contribution of side by side aggregates amounts to only a few percent of the scattered intensity. Figure 1B results from the accumulation of 200 pulses of 2 msec duration with an applied electric field of 5 kV/cm. The relative differences ($\Delta I/I$) resulting from the applied field shown in Fig. 1C indicate a decrease of the scattered intensity by about 40% in the direction parallel to the field and a corresponding increase in the direction perpendicular to the field. This result indicates that in the region of saturation, at high fields, all particles are indeed oriented and illustrates the identity between the electrooptical orientation parameter and the structural order parameter. Note that Fig. 1B corresponds to the continuous transform of an isolated, oriented particle. It is thus different from the pattern of an oriented gel, where the transform is

M. H. J. Koch, E. Dorrington, R. Kläring, A. M. Michon, Z. Sayers, European Molecular Biology Laboratory, c/o DESY, D-2000 Hamburg 52, Federal Republic of Germany.
R. Marquet and C. Houssier, Laboratoire de Chimie Macromoléculaire et Chimie Physique, Sart Tilman, Université de Liège, B-4000 Liège, Belgium.